



Numerical Simulation of 35kV Oil-Immersed Transformer Fire and Extinguishing Effects of High-Pressure Fine Water Mist

Haowei Yao^{1,2*}, Kefeng Lv^{1,2}, Zhangfang Shi³, Youxin Li^{1,2}, Mengyang Xing^{1,2}, Huaitao Song^{1,2}, Wei Ren⁴

¹ College of Building Environment Engineering, Zhengzhou University of Light Industry, Zhengzhou 450001, China

² Zhengzhou Key Laboratory of Electric Power Fire Safety, Zhengzhou 450001, China

³ Emergency Rescue Center of Zhongyuan Oil Field, Puyang 457000, China

⁴ Henan Provincial Scientific Research Platform Service Center, Zhengzhou 450003, China

Corresponding Author Email: yaohaowei@zzuli.edu.cn

<https://doi.org/10.18280/ijht.410309>

ABSTRACT

Received: 5 March 2023

Accepted: 21 May 2023

Keywords:

oil-immersed transformers, combustion characteristics, PyroSim, fire simulation, temperature field distribution, high pressure fine water mist

Oil-immersed transformer is the key equipment of power transmission, the fire caused by its failure will cause huge economic losses. The aim of this study is to investigate the combustion characteristics of oil-immersed transformer fires under different environmental conditions, and the effectiveness of high-pressure fine water spray on transformer fires under different parameters. Numerical simulation of transformer fires using PyroSim software simulation of high-pressure fine water mist fire extinguishing effect - parameter optimisation, focusing on the combustion characteristics of transformer fires at different ambient temperatures (-5°C, 0°C, 5°C, 10°C, 20°C) and wind speeds (0 m/s, 1 m/s, 2 m/s, 4 m/s) and the suppression effect of high-pressure fine water mist on transformer fires at different spray flows (0.3 L/min, 0.6 L/min) and ambient wind speeds (0 m/s, 1 m/s, 2 m/s, 4 m/s). The simulation results show a negative correlation between the temperature variation above the flame and the spatial height. Changes in ambient temperature with insignificant changes in flue gas concentration and mean changes in flue gas temperature between 800°C and 900°C. Changing the ambient wind speed deflects the flame along the wind direction and has a greater effect on the temperature field distribution above the flame. When the spray flow rate is 0.6L/min, the high-pressure fine water mist system has a better cooling effect on transformer fires. This study has shown that high pressure fine water mist systems can effectively extinguish oil-immersed transformer fires under the appropriate parameters. However, the effectiveness of the high-pressure fine water mist in extinguishing fires is reduced in the presence of increased ambient wind speeds. This paper provides the corresponding theoretical support for the development.

1. INTRODUCTION

Transformers are devices that change the AC voltage according to the electromagnetic inductive principle and can be divided into oil-immersed transformers and dry-type transformers according to the cooling method. Oil-immersed transformers are widely used in power engineering because of their strong heat dissipation, low manufacturing and maintenance costs, and ease of recycling [1-5]. Insulation oil is the main insulating and cooling medium for oil-immersed transformers, which are filled with large quantities of combustible transformer oil inside and on top of the oil pillow. Oil-immersed power transformers in the long-term operation process, its internal insulating oil paper will be affected by electrical, thermal, mechanical stress and other factors and gradually deteriorate, resulting in its insulation performance decline, in the fault, high temperature conditions fire, often leading to oil-immersed transformers themselves and other adjacent electrical equipment damage, serious damage to substations, once a fire will not only affect the safe and stable operation of the power grid, and even to the safety of society has a great impact [6-12]. In a 220kV transformer fire true type experiment, the temperature around the fire was up to 800°C,

causing serious damage to the facilities around the substation [13]. Therefore, transformer safety and security is an issue that cannot be ignored.

High pressure fine water mist is a water-based fire extinguishing system which works by using water transformed into water mist by high pressure nozzles. The water mist suppresses fires by displacing oxygen from the gas to asphyxiate the fire source and by cooling the fire through droplet-attenuated radiation. It also creates a protective zone around the source of the fire and provides better insulation against electrical equipment fires. As a result, fine water mist fire extinguishing systems are often used to extinguish incidents such as transformer fires [14-16]. Today, fine water mist fire extinguishing systems are widely used to suppress fires in buildings and industrial rooms. In addition to the environmental friendliness of water, this fine water mist spray has potential advantages, such as: small water consumption for fire extinguishing, little damage to protected areas and fast extinguishing speed [17]. In the fire test of the energy storage power plant, the high pressure fine water mist has a more obvious effect on the suppression of fire, can extinguish the battery fire in a short time, and has a more obvious effect on the fire temperature reduction. So fine water mist has a good

application prospect for power equipment fires [18].

In recent years, the study of numerical simulation of fire extinguishing processes and calculation of fire extinguishing results has been rapidly developed [19]. PyroSim software simulations reduce the effort and cost of testing and the environmental pollution caused by combustion products should also be reduced. Many studies have applied the FDS (Fire Dynamics Simulator) model to high-pressure fine water mist systems. Sikanen et al. [20] used FDS to model three single-hole and five multi-hole spray nozzles for a fine water mist fire suppression system. The ability of FDS to predict the effect of droplet size, velocity, mist flux and number distribution in the spray cone on fire suppression was evaluated. Iqbal et al. [21] investigated the characteristics of water mist produced by single-hole and multi-hole high-pressure jet nozzles, based on the flux density distribution of the spray. Full-scale experiments were conducted and the volumetric flux density distribution of the spray was measured. The numerical results of the distributions were compared with those obtained experimentally, using FDS to model the spray. Chen et al. [22] used the computational fluid dynamics software Fluent to analyse the effect of pressure on the characteristics of the fine water mist field, the study found that the most fine water mist particles below the nozzle, and with the increase in horizontal distance from the nozzle, the number of mist particles becomes less.

This study focuses on the fire combustion characteristics of 35 kV transformers at different ambient temperatures and wind speeds, and the effect of high pressure fine water mist fire extinguishing systems on the fire extinguishing effect of 35 kV transformers at different setting parameters and ambient wind speeds. By means of numerical simulation analysis, the temperature above the fire source, the temperature in the upper layer of the smoke layer and the smoke concentration are analysed. This in turn provides the corresponding theoretical support for the development of high-pressure fine water mist fire extinguishing systems and transformer safety protection.

2. THEORETICAL ANALYSIS

PyroSim uses the equations of conservation of energy, conservation of mass and conservation of momentum for the simulation of the model in order to make the results more accurate. The software divides the set space into a number of small 3D rectangular control bodies or computational cells. Using the equations of conservation of mass, momentum and energy, the division is carried out to calculate the thermal radiation, turbulence in fluid flow in each grid by the finite volume method, and to track and predict the generation and movement of flames and smoke and combine this with the properties of the flaming material to calculate the propagation and spread of the fire.

The equations for the conservation of mass, momentum and energy of the fluid used in the calculations are as follows [23-25]:

Law of Conservation of Mass:

$$\frac{\partial \rho}{\partial \tau} + \nabla \cdot (\rho \mathbf{u}) = 0 \quad \left(\nabla = \left(\frac{\partial}{\partial x}, \frac{\partial}{\partial y}, \frac{\partial}{\partial z} \right) \right) \quad (1)$$

$\mathbf{u} = (u, v, w)^T$

where, ∇ is the operator symbol for a vector, ρ is the gas density (kg/m^3), \mathbf{u} is the velocity vector (m/s).

Law of conservation of momentum:

$$\frac{\partial}{\partial t} (\rho \mu) + \nabla \cdot \rho \mu + \nabla p - \rho g = f + \nabla \cdot \tau_{ij} \quad (2)$$

where, τ is the viscous stress tensor (Pa), g is the acceleration of gravity (m/s^2), μ is the coefficient of dynamic viscosity ($Pa \cdot s$), p is pressure.

The law of conservation of energy:

$$\frac{\partial}{\partial \tau} (\rho h) + \nabla \cdot \rho h \mathbf{u} = \frac{D\rho}{Dt} + q^m - \nabla \cdot q + \Phi \quad (3)$$

where, h is enthalpy (J/kg), q^m is volumetric heat source (W/m^3), q is thermal radiation flux, Φ Dissipation functions (W/m^3).

The energy dissipation factor is essentially negligible compared to the actual rate of heat release in the event of a fire, so Φ can be taken as zero. Then the above equation can be changed to Eq. (4):

$$\frac{\partial}{\partial \tau} (\rho h) + \nabla \cdot \rho h \mathbf{u} = \frac{D\rho}{Dt} + q^m - \nabla \cdot q \quad (4)$$

Eq. (5) is an equation describing the relationship between the macroscopic thermodynamic parameters of a fluid:

$$F(p, \rho, T) = 0 \quad (5)$$

The gas equation of state for an ideal gas is as follows in Eq. (6):

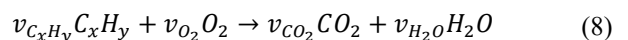
$$p = \frac{\rho RT}{M} = \rho RT \sum_s \frac{Y_s}{M_s} \quad (6)$$

where, Y_s indicates component mass fraction (kg/kg), T is the temperature of the gas ($^{\circ}C$), R is the universal gas constant $8.31 J/(mol \cdot K)$, M is the molecule of the gas (kg/mol), M_s is the molecular weight of the component (kg/mol).

For infinitely fast reactions, the reactants become product species in a fixed grid cell at a rate determined by the characteristic mixing time. The rate of heat release per unit volume is defined by multiplying the rate of mass production of the set of total species by their respective heats of formation. As in Eq. (7) below:

$$\dot{q}''' = - \sum_{\alpha} m_{\alpha}''' \Delta h_{f,\alpha} \quad (7)$$

In fire simulation, a mixed component combustion model is sufficient if only flame combustion effects are considered. If the concentrations of smoke and gases such as carbon dioxide and carbon monoxide generated in a fire are also to be studied, a model of the finite chemical reactions has to be added to the calculations. The usual simplified equation for the combustion of hydrocarbons such as oil is equation [26]:



The rate at which the chemical reaction takes place is:

$$\frac{d(C_xH_y)}{dt} = -A(C_xH_y)^a (O_2)^b e^{-\frac{E}{RT}} \quad (9)$$

where, A is the activation energy reaction finger prefactor, ν is the chemical reaction coefficient, E is the activation energy of the reaction J/mol , R is the molar gas constant, taken as $8.314 J/(mol \cdot K)$, T is the thermodynamic temperature (K), a and b are reaction coefficients.

In the FDS (fire dynamics simulator) software, the cumulative volume distribution of the liquid spray from the nozzle can be represented by the union of two distribution functions, log-norma and Rosin-Rammler [27].

$$F(D) = \begin{cases} \frac{1}{\sqrt{2\pi}} \int_0^D \frac{1}{\sigma D'} e^{-\frac{[\ln(\frac{D'}{d_m})]^2}{2\sigma^2}} dD' & (d_m \geq D) \\ 1 - e^{-0.693(\frac{D}{d_m})^\gamma} & (d_m < D) \end{cases} \quad (10)$$

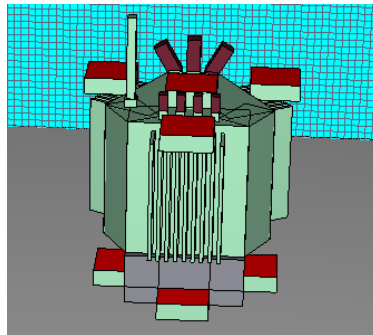
where, D' is the droplet diameter (μm). D is the upper limit of the droplet size interval (μm), d_m is the average droplet diameter, as a function of the nozzle's outlet aperture, working pressure and geometry (μm), When fitting the fine water mist particle size distribution, the empirical constant σ and γ are related by the equation $\sigma = \frac{2}{\sqrt{2\pi}(\ln 2)^\gamma} = \frac{1.15}{\gamma}$.

The movement of the water droplets released when the nozzle is activated can be expressed by the following equation:

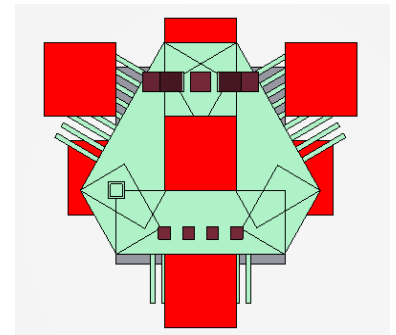
$$\frac{d(m_d u_d)}{dt} = m_d - \frac{1}{2} \rho C_d \pi r_d^2 (u_d - u) |u_d - u| \quad (11)$$



(a) Physical drawing of 35 kV oil-immersed transformer



(b) 35 kV oil-immersed transformer model



(c) Top view of the model

Figure 1. Diagram of 35 kV oil-immersed transformer

Table 1. Description of working conditions

Conditions	Description
1	Comparison at different ambient temperatures (-5°C, 0°C, 5°C, 10°C, 20°C)
2	Comparison at different ambient wind speeds (0 m/s, 1 m/s, 2 m/s, 4 m/s)
3	Different injection flow rates (0.3 L/min, 0.6 L/min)
4	With spraying-different ambient wind speeds (0 m/s, 1 m/s, 2 m/s, 4 m/s)

In this numerical simulation, two conditions of transformer fire simulation are set up, condition 1 is the simulation under different ambient temperatures, the simulation of transformer fire at ambient temperatures of -5°C, 0°C, 5°C, 10°C and 20°C is carried out to analyse the combustion characteristics of transformer fire under different ambient temperatures. Condition 2 is a simulation with different applied wind speeds, comparing the combustion effect of a transformer fire without

where, m_d is the mass of a single water droplet (kg), ρ is the density of water (kg/m^3), C_d is the coefficient of resistance to the movement of water droplet in gas, r_d is the radius of the water droplet (μm), u_d is the velocity of the water droplet movement (m/s), $u_d = \frac{dx_d}{dt}$, x_d is the spatial position of the water droplet in the airflow field at any given moment (m), u is the airflow velocity.

3. MODEL SETUP

3.1 Geometric model

(1) Parameter setting

This article presents a full-scale simulation of a 35 kV transformer fire in order to analyse the combustion characteristics of a transformer fire under different boundary conditions. In the model, the initial ambient temperature is 10°C, the flame burning time is 180 s, the heat release rate per unit area is 2000 kW/m² and the area of the fire source: 0.3m×0.3m.

(2) Measurement point setting

In this simulation environment, a total of eight fire points were set up to simulate a three-dimensional transformer fire, with thermocouple measurement points set above the fire source and smoke concentration measurement devices set at 2.18 m and 2.58 m above the fire source, Figure 1 shows the physical and simulation model of the transformer.

applied wind speed and with wind speeds of 1 m/s, 2 m/s and 4 m/s, as shown in Table 1.

3.2 Grid independence analysis

In numerical simulation research, the grid density is the basis of the simulation calculation, the accuracy of the simulation calculation is closely related to the grid density, the finer the grid density, the more accurate the calculation results. D^*/δ_x is generally used in the study to express the fire feature accuracy, D^* is the fire feature diameter, δ_x is the grid size, and D^* is calculated as follows [28, 29]:

$$D^* = \left(\frac{Q}{\rho_0 C_p \sqrt{g T_0}} \right)^{\frac{2}{5}} \quad (12)$$

where, Q is the power of the fire source (kW), ρ_0 is the air density (kg/m^3), generally taken as $1.29 kg/m^3$, C_p is the

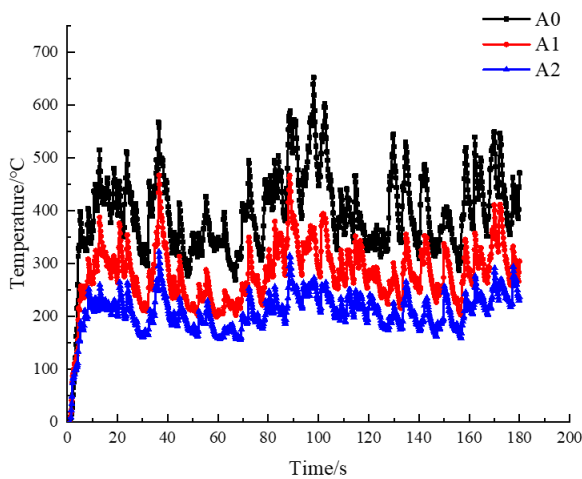
specific heat capacity of air ($\text{kJ}/(\text{kg} \cdot \text{K})$), generally taken as $1.005 (\text{kJ}/(\text{kg} \cdot \text{K}))$. g is the acceleration of gravity (m/s^2), usually $9.8(\text{m}/\text{s}^2)$. T_0 is the ambient temperature (K), here taken as 273 K [30]. The power of the fire source set in this simulation is 180 kW , and $D^* \approx 0.483$ can be calculated, which is more accurate when the value of the dimensionless parameter is in the range of $4\sim 16$ [31]. When the grid size is 0.05 we can get $D^*/\delta_x \in (4\sim 16)$, therefore, in this model, the grid size is taken as $0.05 \times 0.05 \times 0.05$.

4. ANALYSIS OF SIMULATION RESULTS

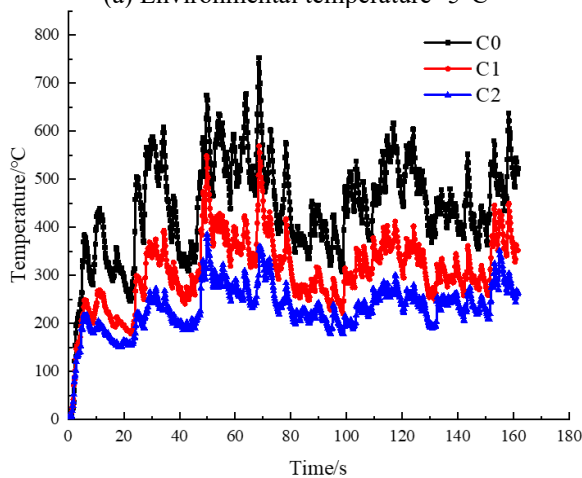
4.1 Analysis of the combustion characteristics of 35 kV transformer fires at different ambient temperature

(1) Effect of different ambient temperatures on the fire temperature of 35 kV transformers

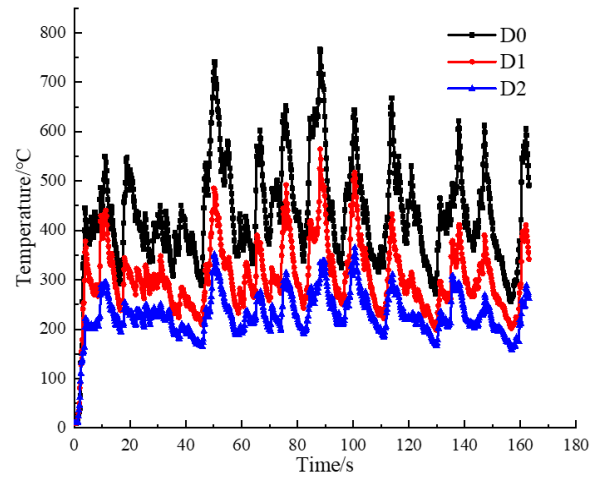
Figure 2 shows the curve of the temperature gradient in the space above the fire source at different ambient temperatures. A, B, C and D are the measured points of the temperature change at the same location above the fire source at different ambient temperatures. From Figure 2, it can be found that the temperature change above the fire source is negatively correlated with the spatial height, with the maximum temperature of the flame at around 700°C . Along with the ambient temperature, the maximum temperature of the flame is around 800°C when the ambient temperature is 5°C , 10°C and 20°C . It can be found that the rise in ambient temperature increases the undulation of the flame burning temperature to some extent, but the overall trend is essentially the same.



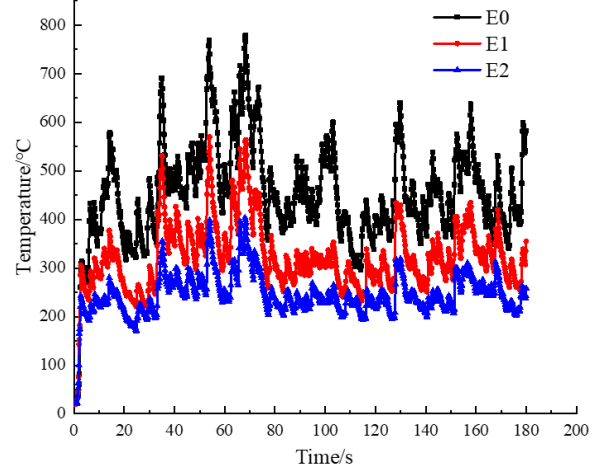
(a) Environmental temperature -5°C



(b) Environmental temperature 5°C



(c) Environmental temperature 10°C

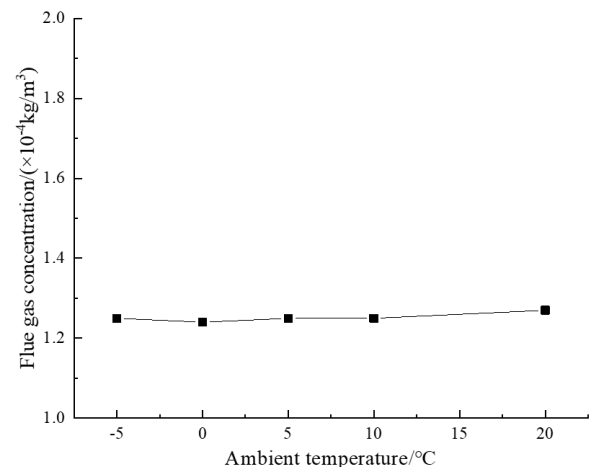


(d) Environmental temperature 20°C

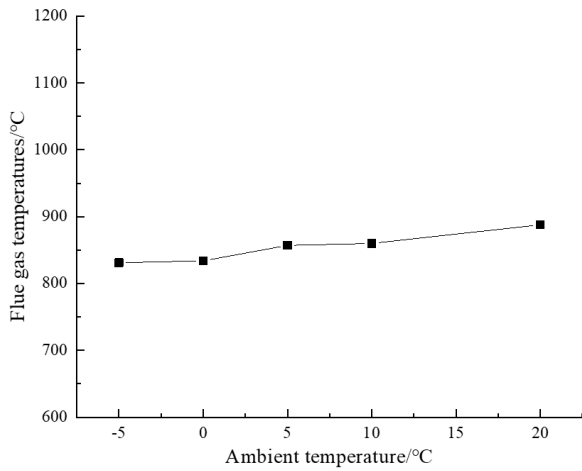
Figure 2. Comparison of temperature above the ignition source under different environmental temperatures

(2) Analysis of flue gas concentration change

From Figure 3, it can be found that the trend of temperature variation of flue gas concentration at different ambient temperatures is basically the same. Taking the average value of the flue gas concentration variation between 60-140s during the stabilisation phase, the flue gas concentrations from flame combustion at different ambient temperatures ($-5, 0, 5, 10$ and 20°C) are $1.25 \times 10^{-4} \text{ kg}/\text{m}^3$, $1.24 \times 10^{-4} \text{ kg}/\text{m}^3$, $1.25 \times 10^{-4} \text{ kg}/\text{m}^3$, $1.25 \times 10^{-4} \text{ kg}/\text{m}^3$, $1.27 \times 10^{-4} \text{ kg}/\text{m}^3$, it can be found that the flue gas concentration changes are basically the same.



(a) Comparison of flue gas concentrations at different ambient temperatures

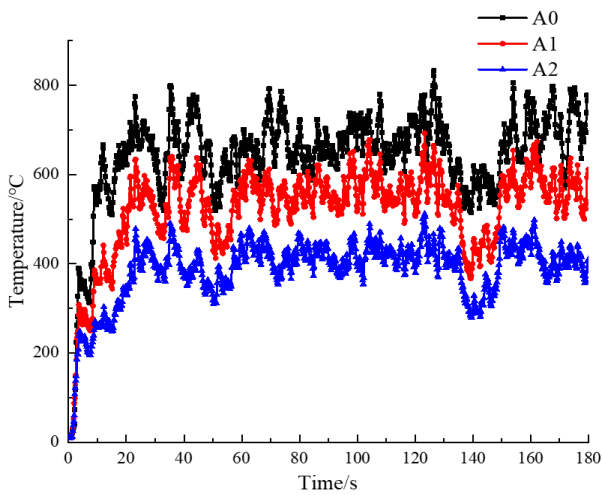


(b) Comparison of flue gas temperatures at different ambient temperatures

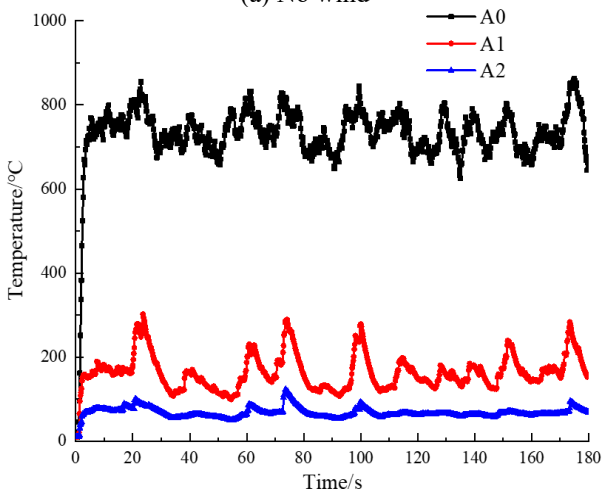
Figure 3. Comparison of flue gas concentrations at different ambient temperatures

Comparison of flue gas temperatures shows that as the ambient temperature rises, there is a certain degree of increase in flue gas temperature, but the temperature changes are all between 800-900°C. From this it can be found that there is little effect on the flue gas by changing the ambient temperature.

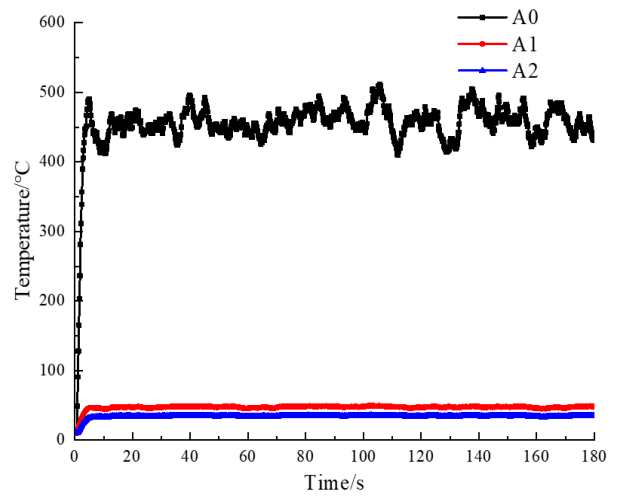
4.2 Analysis of the combustion characteristics of 35 kV transformer fires under different ambient wind speeds



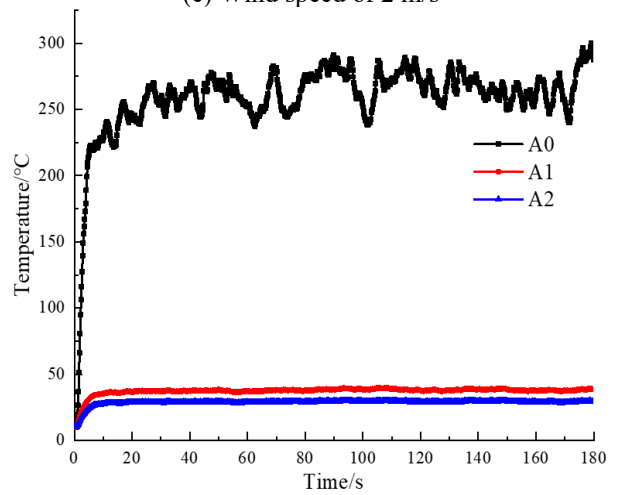
(a) No wind



(b) Wind speed of 1 m/s



(c) Wind speed of 2 m/s



(d) Wind speed of 4 m/s

Figure 4. Comparison of flame temperatures at different ambient wind speeds

(1) Flame temperature analysis

Figure 4 shows the temperature variation curve above the flame at different ambient wind speeds, in which A0-A2 are axial temperature detection points at 0.13 m, 0.43 m and 0.73 m above the flame, measuring the temperature variation at this height.

From Figure 4, it can be found that when there is no applied wind speed, the flame temperature varies in a gradient, with the highest temperature at A0 at around 800°C, and A1 and A2 at around 600°C and 400°C respectively. When the ambient wind speed is 1m/s, the temperature at A0 does not change significantly compared to when there is no wind, but at this time, it can be found that there is a significant decrease in the temperature of temperature measurement points A1 and A2, at this time, the temperature of A1 and A2 is around 200°C and 100°C. It can be learned that compared to the windless condition, when the ambient wind speed is 1m/s, the flame undergoes a certain degree of deflection under the influence of wind speed, compared to A1 and A2, as the A0 point is still inside the flame. The temperature change at measurement point A0 is therefore insignificant and the heat radiation from the flame at measurement points A1 and A2 is reduced due to the deflection of the flame. With the increase of wind speed, it can be found that when the ambient wind speed is 2 m/s and 4 m/s, the temperature of A0 changes from 800°C to 500°C in to 250°C, while the temperature at A1 and A2 has been reduced to below 100°C. It can be noticed that after a certain increase

in wind speed, the flame is already very heavily deflected and the heat radiation to the top of the flame is reduced.

(2) Effect of ambient wind speed on flame pattern

Figure 5 shows the combustion pattern of the transformer fire when burning for 80 s at different ambient wind speeds, it can be found that as the wind speed increases, the flame is deflected to a certain extent with the addition of ambient wind. Combined with the change in flame temperature, the flame burning pattern was axial when there was no wind, when the thermocouples set up were distributed in the flame and the temperature decreased as the distance increased. When there is an ambient wind speed, the flame is deflected in the direction of the wind and some of the thermocouples are exposed to the air without direct contact with the flame as the flame is tilted, so the measured temperature is the flame radiation temperature, which is lower than when there is no wind. The greater the wind speed, the greater the degree of tilt.

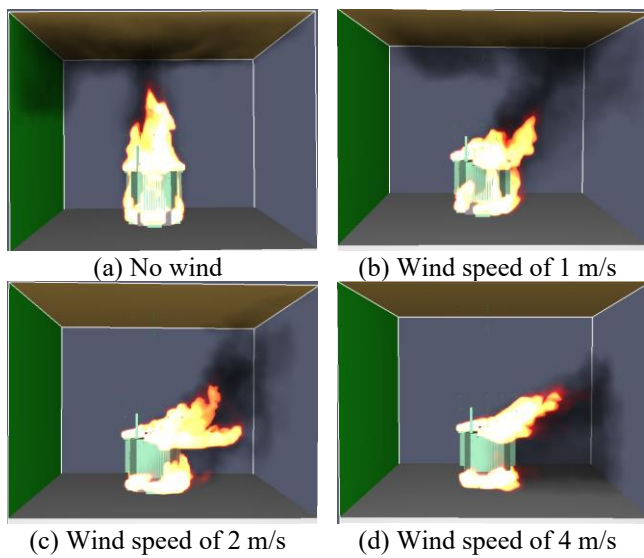


Figure 5. Changes in combustion pattern of transformer fires at different ambient wind speeds

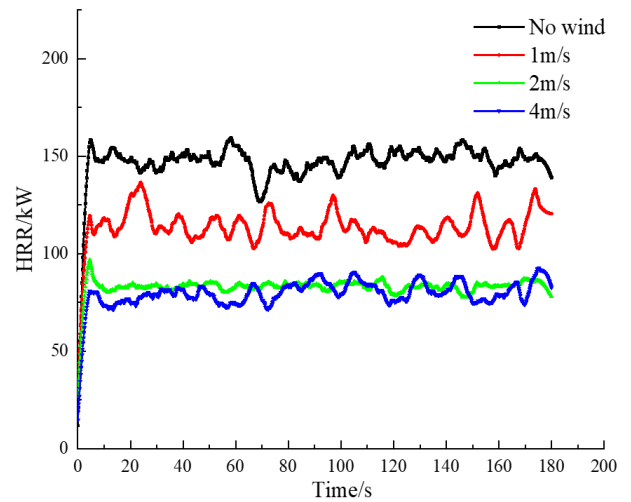
(3) Effect of ambient wind speed on heat release rate and flue gas concentration

From Figure 6(a), it can be found that the heat release rate of a single fire source tends to decrease as the ambient wind speed increases, which suggests that the wind speed has a degree of cooling effect. When there is no wind, the smoke concentration above the flame is around $1.25 \times 10^{-4} \text{ kg/m}^3$ and the smoke temperature is around 600°C . When the ambient wind speed is 1 m/s , the smoke concentration decreases to $1.66 \times 10^{-5} \text{ kg/m}^3$ and the smoke temperature decreases to around 30°C . Combining the results obtained in Figure 6(b) and Figure 6(c), when the wind speed increases to a certain level, the roof of the simulated space is no longer smoke-free and smoke cannot collect on the roof with the flow of wind, thus it can be found that when additional ambient wind speed is added, the ambient wind will blow the smoke away and the effect on the concentration and temperature of the smoke is very obvious.

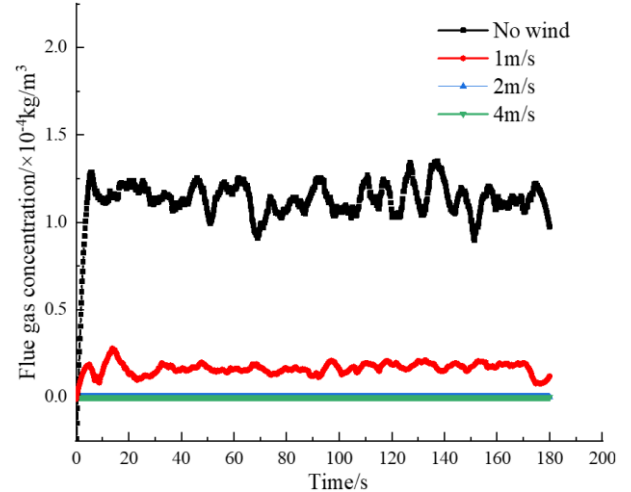
4.3 Effect of different spray flow rates on the effectiveness of high-pressure fine water mist fire extinguishing

When the sprinkler flow varies, the temperature above the flame goes through a period of rapid growth before the sprinklers are turned on and then enters a steady state. Before

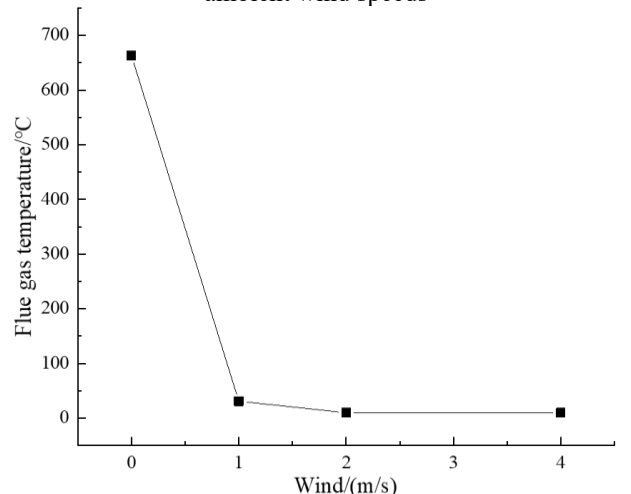
the sprinklers were switched on, the flame temperature was around 500°C . When the sprinkler is turned on, as can be found in Figure 7, the temperature above the flame are a certain degree of decline, the nozzle flow increase is actually a change in the size of the nozzle spray hole, the spray hole increases in the same spray pressure, the spray flow also increases.



(a) Variation curve of heat release rate from a single fire source at different ambient wind speeds



(b) Variation curve of flue gas concentration at different ambient wind speeds



(c) Variation in flue gas temperature at different ambient wind speeds

Figure 6. Plot of the effect of ambient wind speed on heat release rate and flue gas

After the spraying is opened, if the nozzle flow increases in the right amount, the nozzle spray out of the water droplet particle size increases, while the density of water per unit volume also increases, at this time the water medium through heat transfer and thermal convection of the way to absorb heat increases, so the temperature above the fire source is reduced trend, while the effect of atomization of water due to high-pressure water fine water mist system, so that the spray of water mist around the fire to form a water mist, on the one hand, played a cooling cooling effect, on the other hand, through the fog particles on the fire surroundings, isolated from oxygen, and thus play the effect of asphyxiation. Compared to the spray flow rate of 0.3 L/min, the high-pressure fine water mist system has a better cooling effect on transformer fires when the spray flow rate is 0.6 L/min.

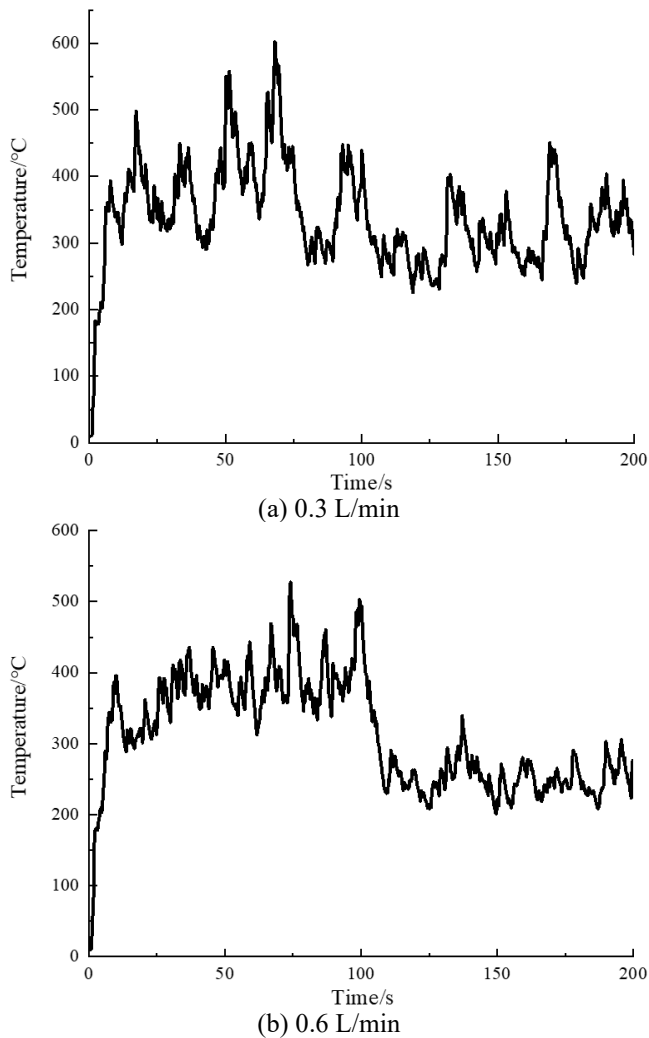


Figure 7. Temperature variation curve at different injection flow rates

4.4 Effect of different ambient wind speeds on the effectiveness of high-pressure fine water mist fire extinguishing

It can be found in Figure 8 that when there is no wind, the temperature above the flame is around 500°C. When the spray is turned on, the flame temperature is reduced and the high-pressure fine water mist plays a cooling and cooling role. When the wind speed is attached, it can be found that the temperature before and after the spray is turned on has decreased to some extent compared to when there is no wind,

which indicates that when there is wind speed, the wind speed also has a cooling effect on the flame temperature. At the same time, the increase in ambient wind will also blow away the high-pressure fine water mist system in the fire around the formation of a water mist envelope, so that the high-pressure fine water mist system of oxygen asphyxiation and cooling cooling effect is weakened, the fire fighting effect is reduced. When the wind speed is too high, it can also cause the lateral spread of flames, which in turn can cause damage around the fire, so the corresponding wind protection measures for transformers have to be carried out.

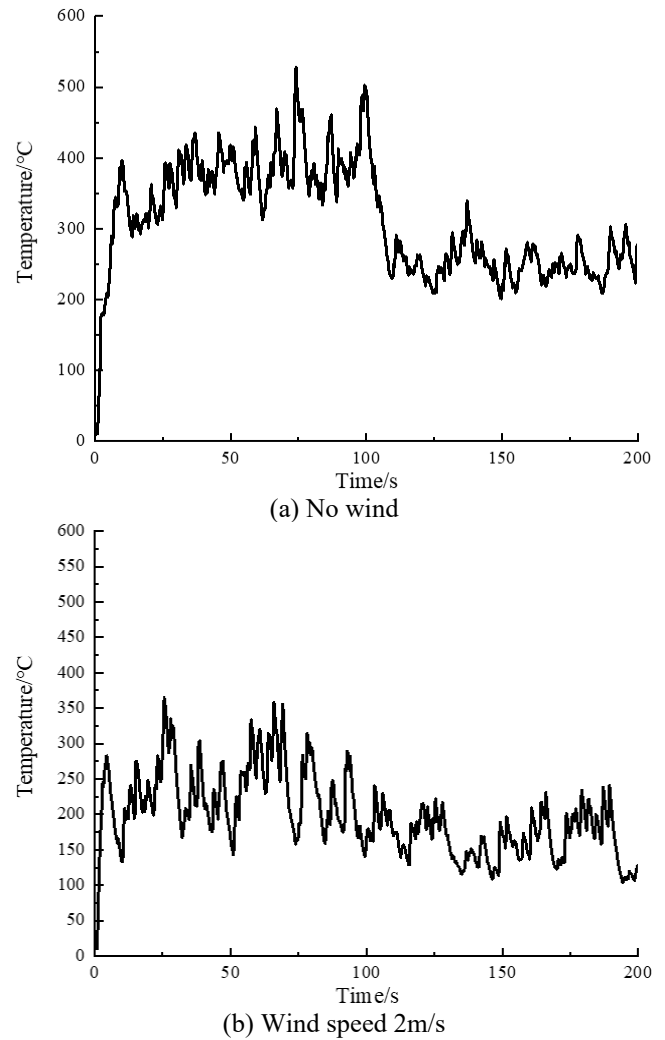


Figure 8. Graph of flame temperature variation at different ambient wind speeds

5. CONCLUSION

This paper analyses 35 kV transformer fires at different ambient temperatures and ambient wind speeds to analyse the changes in flame temperature, smoke concentration and the changes in flame pattern at different ambient wind speeds; and then also analyses the cooling effect of high pressure fine water mist systems on small transformer fires at different jet flows and ambient wind speeds. The results of the analysis are as follows:

(1) In terms of temperature, there is a negative correlation between the change in temperature above the flame and the change in spatial height. Changing the ambient temperature,

as the ambient temperature rises, the flame combustion temperature has ups and downs but does not change much. The flue gas temperature rises to a certain extent, but the average value of temperature changes are between 800°C and 900°C, while the change in flue gas concentration is not obvious. In summary, the effect of ambient temperature on the effectiveness of flame combustion is not significant.

(2) When the ambient wind speed is applied, it can be noticed that the flame burns longitudinally in the absence of wind and shifts in the direction of the wind in the presence of wind, when the heat radiation is reduced. There was little change in temperature at 0.13m above the flame when the ambient wind speed was 1 m/s compared to when there was no wind, and under the same conditions there was a significant drop in temperature at 0.43m and 0.73m above the flame. Continue to increase the ambient wind speed can be found, the flame offset degree increased, the temperature above the flame at different heights have a certain degree of temperature reduction, due to the role of the wind roof smoke is blown by the wind, the roof smoke temperature into the ambient temperature.

(3) When the high-pressure fine water mist system was activated, the temperature of the fire dropped significantly. High-pressure fine water mist cooling is achieved by cooling and oxygen barrier asphyxiation, moderate increase in jet flow, the nozzle sprayed water droplet diameter increases, the possibility of a single drop of water reaching the centre of the flame increases, while the density of water per unit area increases, the water mist on the flame cooling and oxygen barrier asphyxiation effect is enhanced, the adsorption and dilution of flue gas concentration also increases. In the presence of ambient wind speed after the opening of high-pressure fine water fog, high-pressure fine water fog fire extinguishing effect is reduced, because the ambient wind will blow away the formation of high-pressure fine water fog field, which in turn makes its oxygen barrier asphyxiation and cooling effect weakened. Also when the wind speed is too high it can cause a lateral deflection of the flames, which in turn may have an impact around the fire, so it is important to strengthen the wind protection measures for the transformer.

ACKNOWLEDGEMENTS

This work was supported by Henan Province Science and Technology Research Plan Project (Grant No.: 232102321094), Zhengzhou City Collaborative Innovation Special Project (Cultivation of Major Projects) (Grant No.: 2021ZDPY0108), Science and Technology Plan Project of Henan Fire Rescue Corps (Grant No.: 2021XFYY11) and Zhengzhou University of Light Industry Xingkong Maker Space Incubation Project (Grant No.: 2023ZCKJ210).

REFERENCE

- [1] Wang, Y.L., Li, C.H., Zhang, J.Q., Shang, F.J., Chen, S.X., Fan, M.H., Wang, L.F. (2019). Fire accident characteristics and fire extinguishing countermeasures of oil-immersed transformer. *Safety and Environmental Engineering*, 26(6): 166-171. <https://doi.org/10.13578/j.cnki.issn.1671-1556.2019.06.025>
- [2] Chen, Q.W., Xi, D., Hong, W.Y., Hao, X. (2022). Development of intelligent fire fighting device for oil-immersed transformer fire in transformer substation. *Fire Science and Technology*, 41(4): 533-537.
- [3] Martin, D., Beckett, C., Brown, J., Nielsen, S. (2019). Analysis and mitigation of Australian and New Zealand power transformer failures resulting in fires and explosions. *IEEE Electrical Insulation Magazine*, 35(6): 7-14. <https://doi.org/10.1109/MEI.2019.8878255>
- [4] Mardani, K., Vretos, N., Daras, P. (2023). Transformer-based fire detection in videos. *Sensors*, 23(6): 3035. <https://doi.org/10.3390/s23063035>
- [5] Christina, A.J., Salam, M.A., Rahman, Q.M., Islam, M. A., Wen, F., Ang, S.P., Hasan, S., Voon, W. (2018). Investigation of failure of high voltage bushing at power transformer. *Journal of Electrostatics*, 96: 49-56. <https://doi.org/10.1016/j.elstat.2018.09.005>
- [6] Zhang, L.X., Wu, D.Y., Shuai, Y.M., Chen, R., Yang, C. (2022). Property test of oil-immersed insulation paperboard for power transformer. *High Voltage Apparatus*, 58(4): 87-93. <https://doi.org/10.13296/j.1001-1609.hva.2022.04.012>
- [7] Zhang, J., Guo, Y., Yang, T., et al. (2023). Effect of immersion time on the combustion characteristics of oil-impregnated transformer insulating paperboard. *Fire and Materials*, 47(3): 294-304. <https://doi.org/10.1002/fam.3097>
- [8] Yao, H. W., Li, Y.X., Lv, K.F., Wang, D., Zhang, J.G., Zhan, Z.Y., Wang, Z.Y., Song, H.T., Wei, X.G., Qin, H.J. (2023). Numerical simulation analysis of the transformer fire extinguishing process with a high-pressure water mist system under different conditions. *Computer Modeling in Engineering & Sciences*, 136(1): 733-747. <https://doi.org/10.32604/cmescs.2023.022155>
- [9] Ku, Y.H., Zhang, J.G., Wang Z.Y., Li, Y.X., Yao, H.W. (2021). A numerical study on the extinguishing performances of high-pressure water mist on power-transformer fires for different flow rates and particle velocities. *Fluid Dynamics & Materials Processing*, 17(6): 1077-1090. <https://doi.org/10.32604/fdmp.2021.015779>
- [10] Ramaian, T.A.R.P., Maria, S.W.I., Karthik, R. (2017). Performance studies on dielectric and physical properties of eco-friendly based natural ester oils using semi-conductive nanocomposites for power transformer application. *IET Science Measurement & Technology*, 12(3): 323-327. <https://doi.org/10.1049/iet-smt.2017.0467>
- [11] Montero, A., García, B., Burgos J.C., González-García, C. (2022). Dielectric design of ester-filled power transformers: AC stress analysis. *IEEE Transactions on Power Delivery*, 37(3): 2403-2412. <https://doi.org/10.1109/TPWRD.2022.3145880>
- [12] García, B., Ortiz, A., Renedo, C., García, D.F., Montero, A. (2021). Use performance and management of biodegradable fluids as transformer insulation. *Energies*, 14(19): 6357. <https://doi.org/10.3390/en14196357>
- [13] Wang, M.W., Tao, B., Li, J.W., He, Y.Y. (2020). Experimental study on the effectiveness and safety of water mist in electrical fire fighting. *Fire Science and Technology*, 39(7): 969-972. <http://www.xfkj.com.cn/CN/Y2020/V39/I7/969>
- [14] Li, G.C., Xie, L.K., Liu, G.Q., Zhang, Y., Li, B., Wang, C.H. (2023). Fire hazard assessment of true 220kV transformers in power system. *Safety and Environmental*

- Engineering, 30(3): 51-60.
<https://doi.org/10.13578/j.cnki.issn.1671-1556.20220578>
- [15] Arvidson, M. (2014). Large-scale water spray and water mist fire suppression system tests for the protection of Ro-Ro cargo decks on ships. *Fire Technology*, 50: 589-610. <https://doi.org/10.1007/s10694-012-0312-7>
- [16] Chen, B.H., Deng, J., Sun, Y.C., Li, B., Fang, Z., Tao, L. (2020). Study on electrical insulation performance of water mist for electrical transformer. *Fire Science and Technology*, 39(1): 67-69. <http://www.xfkj.com.cn/CN/Y2020/V39/I1/67>.
- [17] Su, L., Zhang, J., Que, X.G., Wang, Z.H., Liu, G.W. (2014). Research on the numerical simulation of the 110kV transformer fire extinguishing by foam spraying. In 2014 7th international conference on intelligent computation technology and automation, Changsha, China, pp. 587-590. <https://doi.org/10.1109/ICICTA.2014.147>
- [18] Feng, H.J., Zou, L., Zhang, Y.H. (2022). Experimental research on fire suppression of lithium iron phosphate battery module by high pressure water mist and discussion on design. *Water & Wastewater Engineering*, 58(11): 114-119, 123. <https://doi.org/10.13789/j.cnki.wwe1964.2022.07.26.0004>
- [19] Liu, J.Y., Liang, D., Zhao, Z., Dong, W.L. (2011). Progress in research and application of electronic ultrasonic water mist fire suppression technology. *Procedia Engineering*, 11: 288-295. <https://doi.org/10.1016/j.proeng.2011.04.659>
- [20] Sikanen, T., Vaari, J., Hostikka, S., Paajanen, A. (2014). Modeling and simulation of high pressure water mist systems. *Fire Technology*, 50: 483-504. <https://doi.org/10.1007/s10694-013-0335-8>
- [21] Iqbal Mahmud, H.M., Khalid, A.M., Graham, R.T. (2016). Experimental and numerical study of high-pressure water-mist nozzle sprays. *Fire Safety Journal*, 81: 109-117. <https://doi.org/10.1016/j.firesaf.2016.01.015>
- [22] Chen, Q., Wei, X., Chen, G., Li, G., Chen, P. (2020). Research on the atomization characteristics of fine water under different pressure. *Fire Science and Technology*, 39(6): 803-806. <http://www.xfkj.com.cn/CN/Y2020/V39/I6/803>.
- [23] Harish, R., Venkatasubbaiah, K. (2015). Numerical study of water spray interaction with fire plume in dual chambers connected to tall shaft. *Fire Safety Journal*, 74: 1-10. <https://doi.org/10.1016/j.firesaf.2015.03.007>
- [24] Li Q., Tang Z., Fang Z., Yuan, J., Wang, J. (2019). Experimental study of the effectiveness of a water mist segment system in blocking fire-induced smoke and heat in mid-scale tunnel tests. *Tunnelling and Underground Space Technology*, 88: 237-249. <https://doi.org/10.1016/j.tust.2019.03.011>
- [25] Mehaddi R., Collin A., Boulet P., Acem, Z., Telassamou, J., Becker, S., Demeurie, F., Morel, J.Y. (2020). Use of a water mist for smoke confinement and radiation shielding in case of fire during tunnel construction. *International Journal of Thermal Sciences*, 148: 106156. <https://doi.org/10.1016/j.ijthermalsci.2019.106156>
- [26] Wu, S.F., Yuan, Y.P. (2020) Simulation research on suppression and extinguishment of fires in a ship engine room by water mist based on FDS. *Shipbuilding of China*, 61(4): 170-187.
- [27] McDermott, R.J., Forney, G.P., McGrattan, K., Mell, W.E. (2010). Fire dynamics simulator version 6: Complex geometry, embedded meshes, and quality assessment. National Institute of Standards and Technology, NIST, 1018-5.
- [28] Hwang, C.C., Edwards, J.C. (2005) The critical ventilation velocity in tunnel fires-a computer simulation. *Fire Safety Journal*, 40(3): 213-244. <https://doi.org/10.1016/j.firesaf.2004.11.001>
- [29] Lin, C.J., Chuah, Y.K., (2008). A study on long tunnel smoke extraction strategies by numerical simulation. *Tunnelling & Underground Space Technology*, 23(5): 522-530. <https://doi.org/10.1016/j.tust.2007.09.003>
- [30] Liang, R., Dai, S.L., Wen, B. (2022). Simulation study on influence of shaft smoke exhaust vent on smoke flow characteristics of L-shaped high-rise buildings. *Journal of Safety Science and Technology*, 18(8): 135-141. <https://doi.org/10.11731/j.issn.1673-193x.2022.08.020>
- [31] Wu, D., Wang, Y.Q., Luo, J.Y., Li, D.H., Chen, Y.B. (2021). Numerical simulation study on the effect of water mist on the fire extinguishment of the comprehensive pipeline gallery. *Journal of Southwest University of Science and Technology*, 36(2): 49-54. <https://nature.swust.edu.cn/CN/Y2021/V36/I2/49>.